

An Indirect Method to Estimate the Force Output of Triceps Surae Muscle

Jizhou Li¹, *Student Member, IEEE*, Yongjin Zhou^{2*}, *Member, IEEE* and Yong-Ping Zheng³, *Senior Member, IEEE*

Abstract—Estimation of force output generated by human muscle is an essential routine of clinical rehabilitation assessment, and could provide considerable insight into rehabilitation, motor control and robotics. Indirect methods for the estimation of force output could be helpful when a bulky and expensive dynamometer is not on hand. Electromyography has been used in previous studies to quantify it in the literature. However, the force output is a summation of the motor unit action potentials, and thus the contributions and performances of superficial and deep-lying muscles could hardly be separated from each other. In this preliminary study, we applied ultrasonography (US) to explore the feasibility of estimating triceps surae force output during isometric plantar flexion with spatial resolution from superficial to deeper muscles. The local deformations of US images are extracted to represent the morphological changes during force generation. It was found US could be utilized to decently (coefficient of determination at 0.875 ± 0.051 and normalized root mean square error 0.160 ± 0.035) estimate the force output and the measured force by a dynamometer.

I. INTRODUCTION

Quantitative assessment of muscle force output is an essential component of many clinical neurological or physical exams, and could provide considerable insight into rehabilitation, motor control and robotics. However, due to testing of intact human muscle requires that muscle output be measured external to the body, to measured forces produced by muscles during various activities directly is currently infeasible. In general, dynamometers have been widely used to measure muscle forces at different joint angles, and it provide accurate readings of muscle force. But as it is bulky, expensive and inconvenient, researches have been exploring indirect approaches for the assessment of muscle forces, such as mathematical model [1], surface Electromyography (sEMG) [2], intramuscular Electromyography [3], mechanomyography (MMG) [4], combination of sEMG and MMG [5] and 1D axial-transmission ultrasonic method [6].

However, a fundamental limitation of sEMG can preclude an accurate assessment of muscle force. An EMG signal is a summation of the motor unit action potentials, occurring within the detection area of the electrode. The contribution

of the muscle or muscle group cannot be separated out. In other words, there are confusing forces generated by synergistic muscle. In addition, although there have been several studies indeed shown that EMG-based estimation of muscle force can be improved by using multiple bipolar electrodes pairs and with a grid of densely spaced monopolar electrodes [2], this approach could not readily look insight into the activations of deep-lying muscles, such as the vastus intermedius (VI) of the quadriceps muscles (QM) and the soleus (SOL) of the triceps surae (TS). Moreover, it seems infeasible to provide any information about muscle morphology or mechanical aspects.

Ultrasonography, as a non-invasive technique to visualise structures inside the human body, has been widely used in the field of measuring morphology changes of skeletal muscles in both static and dynamic conditions [7]. Different muscle morphological parameters, including muscle thickness [8], [9], pennation angle or fiber orientation [10], [11], fiber length [12], fascicle curvature [13] and cross sectional area [14], have been successfully extracted from ultrasound image sequences to provide valid and automatic methods of characterizing activities of various muscles. Recently, Chen *et al.* [14] investigated the relationship between force level and muscle morphological change (thickness, cross-sectional area and pennation angle) using a combination of sEMG, MMG and ultrasound signals from the rectus femoris muscle. They found that the ultrasound-force relationship was more direct than the MMG/sEMG-force. This motivated us to determine whether the regional deformation could be used to assess muscle force level.

The deformation on the tissue activity may be proven to be a valuable tool to reach a more multifaceted and comprehensive insight into muscle function both in studies using healthy subjects as well as in clinical settings [15]. Magnusson *et al.* [16] developed an automated method of tracking tendinous tissue length changes based on the optical flow algorithm. Li *et al.* [17] developed a framework for the estimation and visualization of longitudinal muscle motion.

Accordingly, an ultrasound approach based on the regional deformation was proposed to assess muscle force level through quantitative ultrasound. The isometric condition was chosen because it is the most common test, as it is the simplest to and reproduce and, because the test conditions is well defined. Potential variations pattern in timing were sought for between the medial gastrocnemius (MG) and SOL.

* Corresponding author: Y. Zhou.

¹ J. Li is with the Department of Electronic Engineering, the Chinese University of Hong Kong, Hong Kong. charliejizhou@gmail.com

² Y. Zhou is with the School of Medicine, Shenzhen Key Laboratory of Biomedical Engineering, Shenzhen University, Shenzhen, China. y.zhou.cn@ieee.org

³ Y-P Zheng is with the Interdisciplinary Division of Biomedical Engineering, the Hong Kong Polytechnic University, Hong Kong. ypzhang@ieee.org

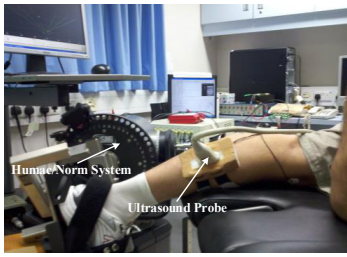


Fig. 1. Experimental setup for collecting the torque/force and ultrasound images during plantar flexion.

II. MATERIALS AND METHODS

A. Subjects and Experimental Protocol

Eight healthy male subjects (mean \pm SD, age= 33.4 ± 5.2 years; body weight= 63.8 ± 10.3 kg; height= 1.65 ± 0.07 m) volunteered to participate in this study. No participant had a history of neuromuscular disorders, and all participants were aware of experimental purposes and procedures. Human subject ethical approval was obtained from the relevant committee in the Hong Kong Polytechnic University, Hung Hom, Hong Kong, and an informed consent was obtained from the subject prior to the experiment.

The testing position of the subject was in accordance with the User's Guide of a Norm dynamometer (Humac/Norm Testing and Rehabilitation System, Computer Sports Medicine, Inc.), as shown in Fig. 1. Each subject was required to put forth his maximal effort of isometric plantar flexion for a period of 3 seconds with verbal encouragement provided. The maximal voluntary contraction (MVC) was defined as the highest value of torque recorded during the entire isometric contraction. Each test was repeated three times with a rest of 5 min between two adjacent trials. Before the actual test, subjects practiced producing a contraction for several times. The MVC torque was then calculated by averaging the two recorded highest torque values from the two tests. The subject was instructed to generate a torque waveform in rough sinusoid shape, up to 90% of his MVC, using ankle plantar flexion movements in prone position. During each contraction, a template and the real-time torque values were shown on a computer screen, as the feedback provided to subjects. The torque was measured by the aforementioned dynamometer and the reason for choosing 90% MVC as the highest value was to avoid muscle fatigue. It should be noted that in such a setup, force output can be achieved from the torque and after normalized into percentages, they exhibits same waveform. The data acquisition procedure was same with our prior work, please see details in [9]. A total of 8 (subjects) \times 200 (frames) \times 3 (trials) ultrasound images with 324×383 pixels were acquired and all the images were cropped to keep the image content only.

B. Ultrasound Approach

Visual inspection of the ultrasound image sequences over time while performing isometric plantar flexion reveals that

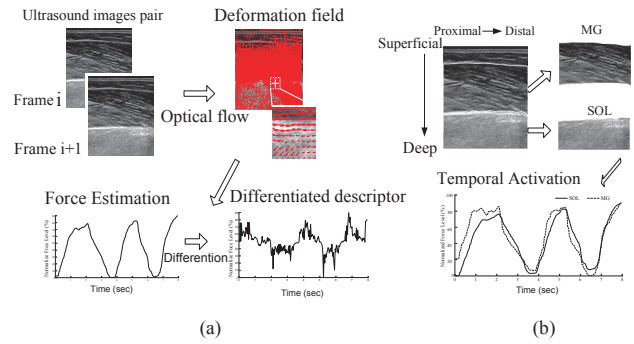


Fig. 2. Scheme of the proposed approach and temporal activation analysis of MG and SOL. (a) A schematic outline of the proposed approach for the force assessment, based on optical flow calculation. (b) Schematic representation of the analysis process for temporal activation of MG and SOL.

the image deformations are highly localized according to anatomy and the joint force level. For instance, when the force increases to reach its MVC and begins to decrease, the moving directions of muscle tissues begin to change to opposite. The local deformation is therefore extracted to present the joint force over time. The calculation process was described below and illustrated in Fig.2 (a).

In this study, a promising optical flow method, named primal-dual algorithm, is implemented to extract the deformation [17], which represents spatio-temporal changes of gray value in the x (from proximal to distal) and y (from superficial to deep) directions, respectively, from ultrasound image sequences during muscle contraction. To further improve the accuracy of the calculation, a coarse-to-fine strategy that builds image pyramids by repeated blurring and downsampling is presented [18]. Optical flow is first computed on the top level (fewest pixels), and then upsampled to initialize the estimation at the next level. Computation at the higher levels in the pyramid involves far fewer unknowns and so is far faster [19].

The estimated force was then approached by averaging regional deformation frame-by-frame in x direction and being normalized over time. Selection of x direction is due to the deformation in y direction extracted from our experiment data is mostly trivial. In this study, we also applied a descriptor as the tempoally-differentiated force changes, as shown in Fig.2 (a).

C. Temporal Activation Analysis

The muscle boundaries of the MG and SOL were manually segmented by defining a piecewise linear boundary in all corresponding ultrasound frames using ImageJ software (ImageJ, National Institutes of Health, USA), as shown in Fig. 2 (b). The approximate regions are outlined as the average manually-measured regions by two investigators. This manual measurement was repeated three times by each investigator.

The force profile of MG (MGF) was defined as the averaged regional deformation in the area of MG, and the force profile of SOL (SOLF) was defined as the averaged

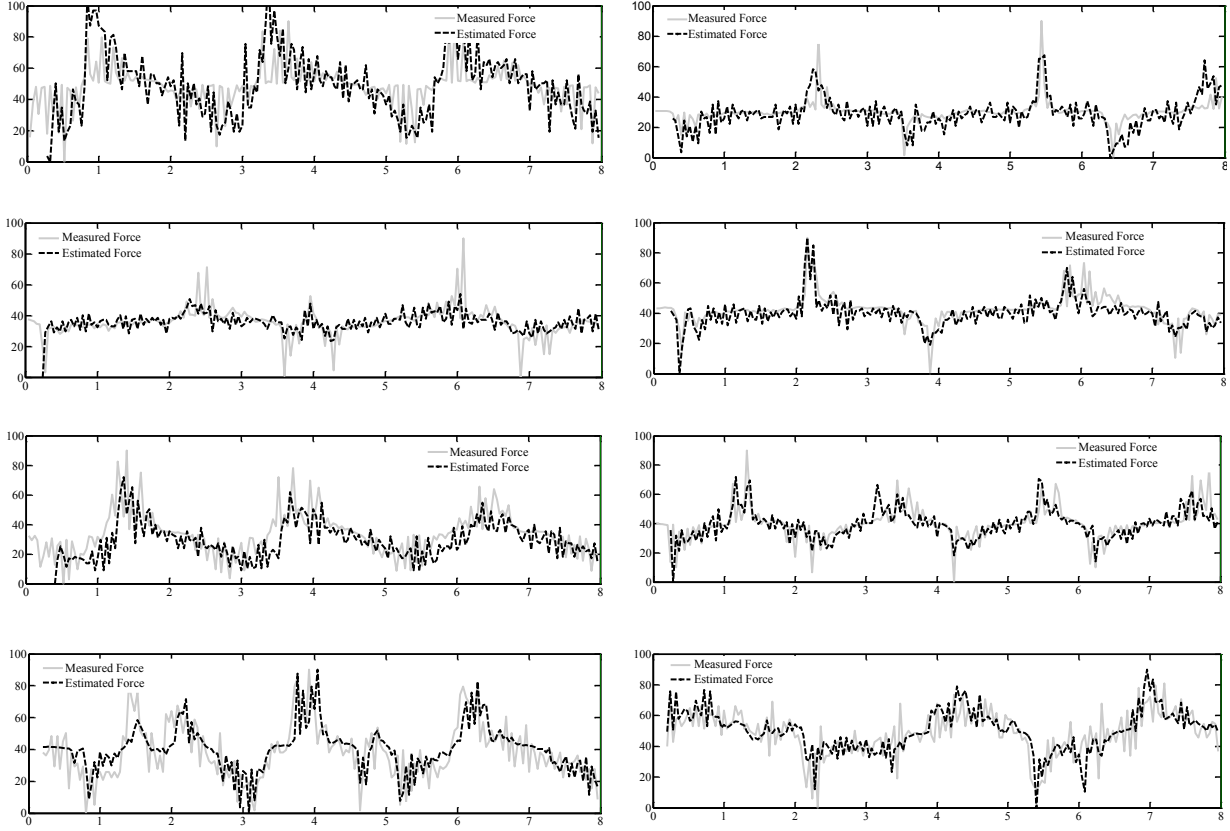


Fig. 3. The results of differentiated force in all subjects. The dashed black line represents the estimated force, while the solid gray line represents the measured force, both temporally-differentiated, while referred to as estimated and measured force respectively.

regional deformation in the area of SOL. Their differences at the corresponding time were treated as their different contribution to the whole force production. One representative result is shown in Fig. 2 (b). Positive value represented the contribution of MG was higher and *vice versa*.

III. RESULTS

A. Accuracy of force estimation

The differentiated force results for all subjects were shown in Fig.3. Overall, there was no significant difference between the Measured Force (MF) and the Estimated Force (EF), though small oscillations of the EF could be seen.

The coefficient of determination (R^2) and the normalized root mean square error (NRMSE) were calculated between the EF and MF to evaluate goodness of fit and the error of estimation. The R^2 was defined as follows:

$$R^2 = 1 - \frac{\sum_{i=1}^N (F_{EF,i} - \overline{F_{MF}})^2}{\sum_{i=1}^N (F_{MF,i} - \overline{F_{MF}})^2} \quad (1)$$

and NRMSE was defined as:

$$NRMSE = \frac{\sqrt{\frac{\sum_{i=1}^N (F_{EF,i} - F_{MF,i})^2}{N}}}{\max(F_{MF}) - \min(F_{MF})} \quad (2)$$

where N , F_{EF} and F_{MF} indicated the total number of data points, the EF and MF, respectively. $\overline{F_{MF}}$ indicated the mean of the MF.

Tab.1 summarised the performance of the estimated force and the differentiated force for all subjects. It could be seen that the R^2 s for the estimated force were higher than 0.819, and the NRMSEs for the estimated force were less than 0.192. The R^2 s for differentiated force in all eight subjects were higher than 0.873, and the NRMSEs are less than 0.152. Overall, the R^2 s and NRMSEs for estimated force were (mean \pm SD) 0.875 ± 0.051 and 0.160 ± 0.035 , respectively. The R^2 s and NRMSEs for differentiated force were 0.917 ± 0.028 and 0.131 ± 0.022 , respectively. Student's t-test yields $p < 0.01$ in all cases.

TABLE I
SUMMARY OF THE PERFORMANCE OF THE ESTIMATED FORCE AND THE DIFFERENTIATED FORCE FOR ALL SUBJECTS.

Subject	Estimated force		Differentiated force	
	R^2	NRMSE	R^2	NRMSE
1	0.853 ± 0.024	0.153 ± 0.035	0.873 ± 0.012	0.152 ± 0.006
2	0.871 ± 0.107	0.172 ± 0.063	0.909 ± 0.071	0.129 ± 0.032
3	0.914 ± 0.038	0.130 ± 0.027	0.934 ± 0.009	0.150 ± 0.019
4	0.912 ± 0.038	0.148 ± 0.025	0.950 ± 0.027	0.103 ± 0.027
5	0.833 ± 0.036	0.171 ± 0.023	0.899 ± 0.024	0.126 ± 0.024
6	0.895 ± 0.023	0.172 ± 0.011	0.909 ± 0.039	0.120 ± 0.019
7	0.899 ± 0.011	0.144 ± 0.036	0.922 ± 0.022	0.124 ± 0.028
8	0.819 ± 0.132	0.192 ± 0.062	0.943 ± 0.016	0.146 ± 0.023
Mean	0.875 ± 0.051	0.160 ± 0.035	0.917 ± 0.028	0.131 ± 0.022

Fig.4 (a) depicted boxplots of the R^2 during ascending ramp and descending ramp, for all eight subjects in three trials. Mean R^2 between the MF and EF was 0.903 ± 0.068 (range: 0.661-0.991) for the ascending ramp and $0.860 \pm$

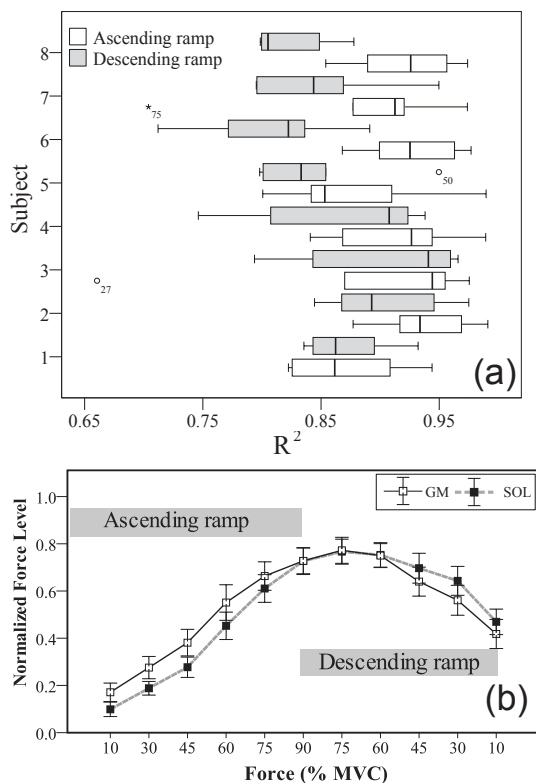


Fig. 4. (a) Comparison of R^2 in ascending ramp and descending ramp. (b) The relationship between averaged MGF and SOLF vs. %MVC. The ascending ramp and descending ramp are indicated with grey horizontal bars.

0.062 (range: 0.712-0.975) for the descending ramp. Fig. 4 (b) depicted the relationship between the MGF and SOLF with respect to specific MVC (10% vs. 30% vs. 45% vs. 60% vs. 75% vs. 90%). There was a difference in MGF and SOLF in the ascending and descending ramps. MGF was higher than SOLF in the ascending ramp (0.069 ± 0.038), and less than SOLF in the descending ramp (0.033 ± 0.035).

IV. DISCUSSION & CONCLUSION

In this study we have explored the ultrasound approach based on local deformation for the muscle force estimation. This preliminary study completed a decent estimation of triceps surae force during isometric plantar flexion. The present data revealed that there was linear relationship between the actual force production and the averaged regional deformation computed using US images. Therefore, the proposed force estimation procedures can be a promising tool to access to the activation pattern of deep-lying muscles non-invasively and individually. Further experiments should be done on a larger number of subjects to further evaluate and improve the proposed procedures.

REFERENCES

[1] R. Ait-Haddou, A. Jinha, W. Herzog, and P. Binding, "Analysis of the force-sharing problem using an optimization model," *Mathematical Miosciences*, vol. 191, no. 2, pp. 111–122, 2004.

[2] D. Staudenmann, D. F. Stegeman, and J. H. van Dieën, "Redundancy or heterogeneity in the electric activity of the biceps brachii muscle? added value of pca-processed multi-channel emg muscle activation estimates in a parallel-fibered muscle," *Journal of Electromyography and Kinesiology*, vol. 23, no. 4, pp. 892–898, 2013.

[3] E. N. Kamavuko, D. Farina, K. Yoshida, and W. Jensen, "Estimation of grasping force from features of intramuscular emg signals with mirrored bilateral training," *Annals of Biomedical Engineering*, vol. 40, no. 3, pp. 648–656, 2012.

[4] C. Orizio, "Muscle sound: bases for the introduction of a mechanomyographic signal in muscle studies," *Critical Reviews in Biomedical Engineering*, vol. 21, no. 3, pp. 201–243, 1992.

[5] W. Youn and J. Kim, "Estimation of elbow flexion force during isometric muscle contraction from mechanomyography and electromyography," *Medical & Biological Engineering & Computing*, vol. 48, no. 11, pp. 1149–1157, 2010.

[6] P. Pourcelot, M. Defontaine, B. Ravary, M. Lemâtre, and N. Crevier-Denoix, "A non-invasive method of tendon force measurement," *Journal of Biomechanics*, vol. 38, no. 10, pp. 2124–2129, 2005.

[7] E. Giannakou, N. Aggeloussis, and A. Arampatzis, "Reproducibility of gastrocnemius medialis muscle architecture during treadmill running," *Journal of Electromyography and Kinesiology*, vol. 21, no. 6, pp. 1081–1086, 2011.

[8] P. Hodges, L. Pengel, R. Herbert, and S. Gandevia, "Measurement of muscle contraction with ultrasound imaging," *Muscle & Nerve*, vol. 27, no. 6, pp. 682–692, 2003.

[9] J. Li, Y. Zhou, Y. Lu, G. Zhou, L. Wang, and Y.-P. Zheng, "Sensitive and efficient detection of quadriceps muscle thickness changes in cross-sectional plane using ultrasonography: A feasibility investigation," *IEEE Journal of Biomedical and Health Informatics*, vol. 18, no. 2, pp. 628–635, 2014.

[10] M. Rana, G. Hamarneh, and J. M. Wakeling, "Automated tracking of muscle fascicle orientation in b-mode ultrasound images," *Journal of biomechanics*, vol. 42, no. 13, pp. 2068–2073, 2009.

[11] Y. Zhou, J. Li, G. Zhou, Y.-P. Zheng *et al.*, "Dynamic measurement of pennation angle of gastrocnemius muscles during contractions based on ultrasound imaging," *Biomedical Engineering OnLine*, vol. 11, no. 63, 2012.

[12] I. D. Loram, C. N. Maganaris, and M. Lakie, "Use of ultrasound to make noninvasive in vivo measurement of continuous changes in human muscle contractile length," *Journal of Applied Physiology*, vol. 100, no. 4, pp. 1311–1323, 2006.

[13] J. Darby, B. Li, N. Costen, I. Loram, and E. Hodson-Tole, "Estimating skeletal muscle fascicle curvature from b-mode ultrasound image sequences," *IEEE Transaction on Biomedical Engineering*, vol. 60, no. 7, pp. 1935–1945, 2013.

[14] X. Chen, Y.-P. Zheng, J.-Y. Guo, Z. Zhu, S.-C. Chan, and Z. Zhang, "Sonomyographic responses during voluntary isometric ramp contraction of the human rectus femoris muscle," *European Journal of Applied Physiology*, vol. 112, no. 7, pp. 2603–2614, 2012.

[15] F. Lindberg, F. Öhberg, L.Å. Brodin, and C. Grönlund, "Assessment of intramuscular activation patterns using ultrasound m-mode strain," *Journal of Electromyography and Kinesiology*, vol. 23, no. 4, pp. 879–885, 2013.

[16] S. Magnusson, P. Hansen, P. Aagaard, J. Brønd, P. Dyhre-Poulsen, J. Bojsen-Moller, and M. Kjaer, "Differential strain patterns of the human gastrocnemius aponeurosis and free tendon, in vivo," *Acta Physiologica Scandinavica*, vol. 177, no. 2, pp. 185–195, 2003.

[17] J. Li, Y. Zhou, K. Ivanov, and Y.-P. Zheng, "Estimation and visualization of longitudinal muscle motion using ultrasonography: A feasibility study," *Ultrasonics*, vol. 54, no. 3, pp. 779–788, 2014.

[18] A. Bruhn, J. Weickert, and C. Schnörr, "Lucas/kanade meets horn/schunck: Combining local and global optic flow methods," *International Journal of Computer Vision*, vol. 61, no. 3, pp. 211–231, 2005.

[19] S. Baker, D. Scharstein, J. Lewis, S. Roth, M. J. Black, and R. Szeliski, "A database and evaluation methodology for optical flow," *International Journal of Computer Vision*, vol. 92, no. 1, pp. 1–31, 2011.